Robotica (2006) volume 24, pp. 377–383. © 2005 Cambridge University Press
doi:10.1017/S0263574705002304 Printed in the United Kingdom

Human arm kinematics for robot based rehabilitation

Matjaž Mihelj

Faculty of Electrical Engineering, University of Ljubljana, Tržaška c. 25, SI-1000 Ljubljana (Slovenia)
E-mail: matjaz.mihelj@robo.fe.uni-lj.si

(Received in Final Form: September 5, 2005, first published online 23 November 2005)

SUMMARY
The paper considers a technique for computation of the inverse kinematic model of the human arm for robot based rehabilitation that uses measurements of the hand position and orientation and radial acceleration of the upper arm. Analytical analysis and empirical validation of the method are presented. The algorithm enables estimation of human arm angles, which can be used in trajectory planning for rehabilitation robots, evaluation of motion of patients with movement disorders, and generation of virtual reality environments.

KEYWORDS: Arm inverse kinematics; Sensor integration; Rehabilitation robotics.

I. INTRODUCTION

Upper-limb rehabilitation systems have been designed for restoring the upper limb functions in individuals with disabilities resulting from spinal cord injury (SCI), stroke and muscle dystrophy. These systems are based either on functional electrical stimulation (FES) or rehabilitation robots and haptic interfaces.[1] Hillman defined rehabilitation robotics as the application of robotic technology to the rehabilitation needs of people with disabilities as well as the growing elderly population.[2] This definition includes augmentative mobility, robots for therapeutic training and robots for help care-givers. On the other hand, haptic interfaces that are also gaining popularity have mostly been used as evaluation devices for assessing the level of disability and the functional improvement during rehabilitation.[3]

In rehabilitation an important issue is the kinematic analysis of limb movement which can be used to assess disability of patients with movement disorders.[4] In this regard it becomes relevant to measure not only the endpoint position of the arm, but also the respective joint angles. Moreover, when applying electrical stimulation to the upper-limb it is important to be aware of the arm configuration to properly select the required stimulation pattern. Therefore, it is necessary to calculate the inverse kinematics of the limb.

The human arm can be modeled as a seven-degree-of-freedom mechanism (Fig. 1) consisting of the shoulder ball–and–socket joint with rotation axes for abduction–adduction (q_1), flexion–extension (q_2), and pronation–supination (q_3) of the upper arm, the elbow double–hinge joint with rotation axes for flexion–extension (q_4), and pronation–supination (q_5) of the forearm and the wrist double–hinge joint with rotation axes for abduction–adduction (q_6), and flexion–extension (q_7) of the hand. For simplification we will consider the elbow pronation–supination rotation as a wrist joint angle, since it only effects the hand orientation and not its position. The shoulder and elbow joints are connected through the upper arm segment with the length l_u, and the elbow and the wrist joints through the forearm segment with the length l_f. The inverse kinematics problem of the human arm can be stated as follows: given the position and the orientation of the hand, find the seven joint angles. Since the given position and the orientation of the hand specify six, rather than seven, independent quantities, the arm is a redundant system, and there are an infinite number of solutions for the joint angles. Therefore, the number of degrees of freedom (DOFs) of the upper extremity is such, that by using a rehabilitation robot attached to the hand, human arm joint angles are neither controllable nor observable.

Several inverse kinematics algorithms have been proposed specifically for the human arm. The workspace of the mechanism was systematically analyzed by Korein.[5] He observed that the first two shoulder joints along with their joint limits restrict the tip of the elbow to lie on a spherical polygon. By intersecting the elbow swivel circle with the polygon it is possible to determine the legal elbow configurations as a function of the joint limits of the first two joints. Additionally, the twist induced by the third joint also restricts the elbow to lie on a circular arc. By taking the intersection of all sets of valid elbow arcs, Korein derived the restrictions on the elbow position by the joint limits. Tolani and Badler[6] proposed an analytic approach. The basic strategy of their approach is to reduce the degrees-of-freedom of the arm by one, so as to make it possible to obtain the closed-form equations that solve the inverse kinematics. The reduction of the degrees-of-freedom is done by fixing one joint angle at its previous value. In other words, when the goal position changes, one of the joint angles still retains its previous value so that the other six joint angles can be obtained analytically. An inverse kinematics approach developed by Koga et al.[7] focuses on generating natural looking arm postures. They use the sensorimotor transformation model proposed by Soechting and Flander[8] to guess a posture for the arm that matches physiological observations of humans. Because the solutions are not exact,

https://doi.org/10.1017/S0263574705002304 Published online by Cambridge University Press

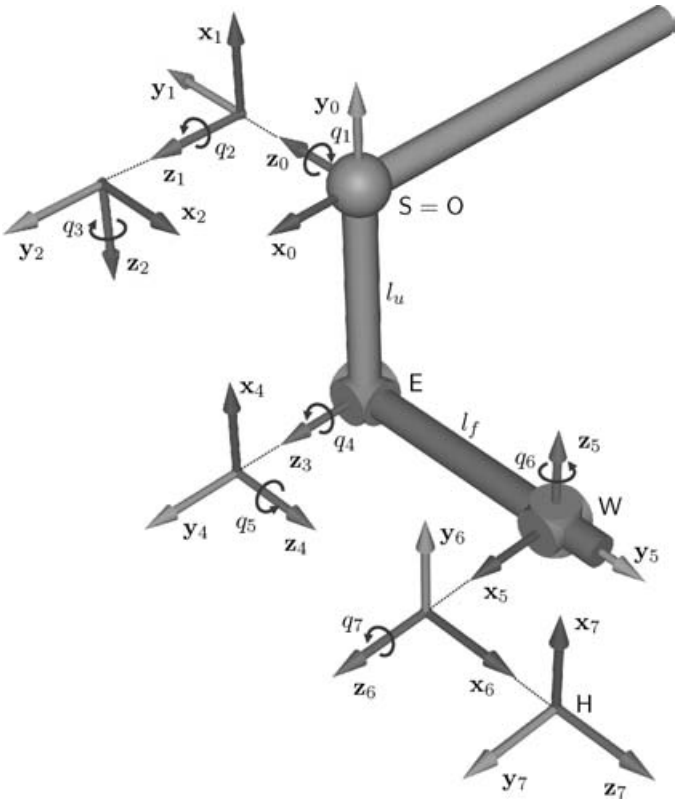


Fig. 1. Simplified human arm kinematics using 7 degrees-of-freedom; joint coordinate systems and rotation axes.

the wrist position of the guessed posture may not be what is desired. Therefore, a pseudoinverse iteration procedure has to be carried out to tune the joint angles till the correct wrist position is obtained. Loftin et al. proposed an algorithm which incorporates the physiological observation that arm and hand postures are, for the most part, independent of each other into the inverse kinematics problem to produce natural looking arm postures without invoking the pseudoinverse Jacobian iterations.[9] This means that it is possible to find the forearm and upper arm posture to match the wrist position and then determine the joint angles for the wrist to match the hand orientation. The arm posture is as in Koga et al.[7] determined by a simple sensorimotor transformation model.

The proposed algorithms give rather inaccurate estimates of the arm posture, which is good enough for graphical presentation and not suitable for use in control systems. In order to be able to adequately measure arm angles a position measurement system is required in addition to the mechanism of the rehabilitation robot or haptic device. This can either be a complex optical measurement system[10] (OPTOTRAK, Northern Digital, Inc., VICON, Vicon Motion Systems, etc.) or a more simple system consisting of flexible goniometers,[11] which are less reliable and more cumbersome. On the other hand, with the use of a rehabilitation robot or haptic device, the position of the attachment point of the mechanism to the human arm is already known from the kinematic model of the device. Therefore, it becomes reasonable to use these existent data with minimal additional measurements to cope with redundant degrees of freedom of the upper extremity.

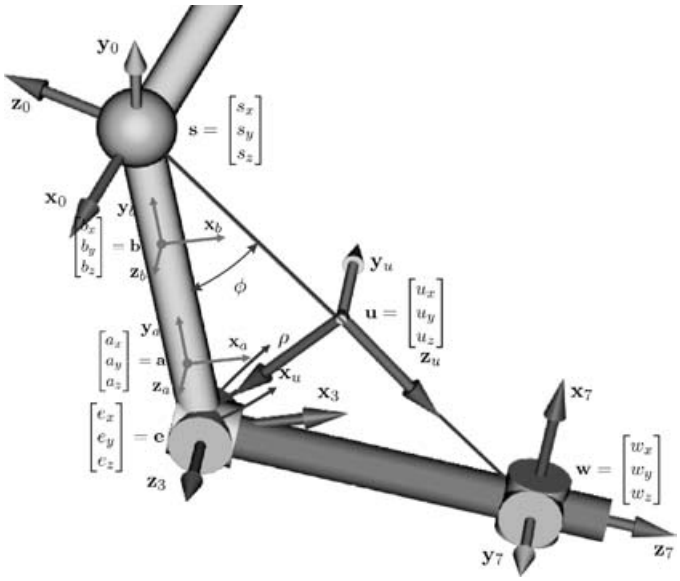


Fig. 2. Estimation of arm angles using hand pose data and upper arm radial acceleration measurements.

II. METHODS

II.1. Inverse kinematics algorithm

The kinematic chain of our interest contains seven joint variables, therefore it has one redundant degree of freedom. A simple physical interpretation of the redundant degree of freedom is based on the observation that if the wrist is held fixed, the elbow is still free to swivel about a circular arc whose normal vector is parallel to the straight line connecting the shoulder and the wrist[12] (Fig. 2).

As already noticed, the exact inverse kinematics cannot be computed unless additional measurements are considered beside measuring the hand position and orientation. The algorithm proposed in this paper uses an extra constraint to estimate the exact elbow position. It will be shown that by measuring the radial acceleration of the upper arm it is possible to estimate one coordinate of the elbow joint, thus constraining the redundant system in a way to allow computation of the inverse kinematics of the arm. Acceleration measurements have already successfully been implemented in the estimation of the angles of lower extremities.[13]

Based on relations in Fig. 1, the following arm transformation matrices can be defined

$$\mathsf{T}_s = Rot(z_0, q_1)Rot(z_1, q_2)Rot(z_2, q_3)Trans(z_2, l_u) \quad (1)$$

$$\mathsf{T}_e = Rot(z_3, q_4)Trans(z_4, l_f) \quad (2)$$

$$\mathsf{T}_w = Rot(z_4, q_5)Rot(z_5, q_6)Rot(z_6, q_7), \quad (3)$$

where T_s, T_e, and T_w are the shoulder, elbow, and wrist transformation matrices respectively. The following transformations determine elbow, E, wrist, W, and hand, H, poses relative to the base coordinate system S

$$\mathsf{E} = \mathsf{T}_s \quad (4)$$

$$\mathsf{W} = \mathsf{T}_s \cdot \mathsf{T}_e \quad (5)$$

$$\mathsf{H} = \mathsf{T}_s \cdot \mathsf{T}_e \cdot \mathsf{T}_w. \quad (6)$$

https://doi.org/10.1017/S0263574705002304 Published online by Cambridge University Press

In Fig. 2, abbreviations **s**, **e** and **w** define positions of shoulder, elbow, and wrist joints relative to the base coordinate frame. Presuming that the shoulder joint position is constant and the base coordinate system is attached in the shoulder joint as is indicated in the Fig. 1, the position of the elbow joint can simply be calculated as a function of shoulder angles q_1 and q_2 and upper arm length l_u as

$$\mathbf{e} = \begin{bmatrix} l_u \sin q_1 \cos q_2 \\ -l_u \cos q_1 \cos q_2 \\ -l_u \sin q_2 \end{bmatrix}. \tag{7}$$

If the position of the shoulder joint is fixed, the radial acceleration (acceleration in the direction of the upper arm segment) at a point $\mathbf{a} = [a_x\ a_y\ a_z]^T$ expressed in the local frame of the upper arm, E (see Fig. 1 and Fig. 2), can be determined as

$$\begin{aligned} \ddot{a}_y = {} & g \cos q_1 \cos q_2 + (l_u - a_y)\left(\dot{q}_1^2 \cos {q_2}^2 + \dot{q}_2^2\right) \\ & + (a_x \sin q_3 + a_z \cos q_3)(\ddot{q}_1 \cos q_2 - 2\dot{q}_2\dot{q}_3) \\ & + (a_x \cos q_3 - a_z \sin q_3)(\ddot{q}_2 + \dot{q}_1(2\dot{q}_3 - \dot{q}_1 \sin q_2)\cos q_2). \end{aligned} \tag{8}$$

Considering that the attachment point of the accelerometer is close to the straight line connecting shoulder and elbow joints, distances a_x and a_z become small and can be neglected. Therefore, simplification of (8) is justified to obtain

$$\ddot{a}_y \approx g \cos q_1 \cos q_2 + (l_u - a_y)\left(\dot{q}_1^2 \cos q_2^2 + \dot{q}_2^2\right). \tag{9}$$

Equation (9) shows that the radial acceleration at the point $\mathbf{a} = [a_x\ a_y\ a_z]^T$ consists of two terms. The gravity generated acceleration $g \cos q_1 \cos q_2$ is independent of the accelerometer position, while the dynamic acceleration, $(l_u - a_y)(\dot{q}_1^2 \cos {q_2}^2 + \dot{q}_2^2)$, depends on the distance between the local frame E attached on the upper arm at the elbow joint and the accelerometer attachment point. In a point where l_u equals a_y the second component vanishes. However, in this case is required positioning of the accelerometer exactly over the shoulder joint, what is relatively impractical. When considering only slow movements the dynamic component of the measured acceleration $\ddot{a}_y$ can be neglected to obtain

$$\ddot{a}_y \approx g \cos q_1 \cos q_2. \tag{10}$$

On the other hand, when also fast movements have to be considered, an additional accelerometer can be used for measuring the radial acceleration of the upper arm in a second point at the location $\mathbf{b} = [b_x\ b_y\ b_z]^T$, relative to the local coordinate frame E to obtain

$$\ddot{b}_y \approx g \cos q_1 \cos q_2 + (l_u - b_y)\left(\dot{q}_1^2 \cos {q_2}^2 + \dot{q}_2^2\right). \tag{11}$$

With a simple algebraic manipulation, it is possible to estimate the e_y coordinate of the elbow joint (2) for slow movements from (10) as

$$e_y = -\frac{\ddot{a}_y l_u}{g} = -l_u \cos q_1 \cos q_2 \tag{12}$$

and generally from (9) and (11) as

$$e_y = \frac{\ddot{b}_y(a_y - l_u) - \ddot{a}_y(b_y - l_u)}{g(b_y - a_y)} = -l_u \cos q_1 \cos q_2. \tag{13}$$

As it is shown next, the e_y coordinate that constrains the elbow position to a horizontal plane, and the measured hand pose are sufficient conditions to compute the arm inverse kinematics.

In order to estimate the arm inverse kinematics the conditions of the swivel of the elbow joint about a circular arc as indicated in Fig. 2 will be analyzed. The normal vector of the swivel arc, $\mathbf{z}_u$, which is parallel to the straight line between the shoulder and the wrist can be computed as

$$\mathbf{z}_u = \frac{\mathbf{w} - \mathbf{s}}{\|\mathbf{w} - \mathbf{s}\|}. \tag{14}$$

The shoulder position, **s**, is assumed to be fixed in space and determined prior to the experiment. On the other hand, the wrist position, **w**, can directly be determined from the robot kinematic model. Based on a simple trigonometry we determine the radius of the swivel arc, ρ, using the angle between the upper arm and the straight line connecting the wrist and the shoulder joints

$$\phi = \arccos \frac{\|\mathbf{w} - \mathbf{s}\|^2 + l_u^2 - l_f^2}{2 l_u \|\mathbf{w} - \mathbf{s}\|} \tag{15}$$

as

$$\rho = l_u \sin \phi. \tag{16}$$

The center of the swivel arc expressed in the base frame can then simply be determined as

$$\mathbf{u} = l_u \mathbf{z}_u \cos \phi. \tag{17}$$

Next, a unit vector $\mathbf{x}_u$ orthogonal to the normal vector of the swivel arc $\mathbf{z}_u$ and pointing from the straight line connecting the wrist and the shoulder joints toward the elbow joint will be defined. The second component, ${}^{(2)}\mathbf{x}_u$, of the vector $\mathbf{x}_u$ can be determined as

$${}^{(2)}\mathbf{x}_u = \frac{e_y - u_y}{\rho}. \tag{18}$$

Since we require vectors $\mathbf{x}_u$ and $\mathbf{z}_u$ to form an orthonormal basis they need to satisfy the following constraints: $\|\mathbf{x}_u\| = 1$ and $\mathbf{x}_u \cdot \mathbf{z}_u = 0$. Considering these constraints it is possible to determine the remaining components, ${}^{(1)}\mathbf{x}_u$ and ${}^{(3)}\mathbf{x}_u$, of the $\mathbf{x}_u$ vector as

$$\begin{aligned} {}^{(1)}\mathbf{x}_u &= \frac{-u_x u_y {}^{(2)}\mathbf{x}_u + u_z \sqrt{\|\mathbf{u}\|^2\left(1 - {}^{(2)}\mathbf{x}_u\right) - u_y^2}}{\|\mathbf{u}\|^2 - u_y^2}, \\ {}^{(3)}\mathbf{x}_u &= -\frac{u_x {}^{(1)}\mathbf{x}_u + u_y {}^{(2)}\mathbf{x}_u}{u_z}. \end{aligned} \tag{19}$$

https://doi.org/10.1017/S0263574705002304 Published online by Cambridge University Press

The orthonormal vector $\mathbf{y}_u$ can simply be determined as a normalized cross product of vectors $\mathbf{z}_u$ and $\mathbf{x}_u$ as

$$\mathbf{y}_u = \frac{\mathbf{z}_u \times \mathbf{x}_u}{\|\mathbf{z}_u \times \mathbf{x}_u\|}. \tag{20}$$

Orthonormal vectors $\mathbf{x}_u$, $\mathbf{y}_u$ and $\mathbf{z}_u$ form a basis of a local coordinate frame U attached at the center of the swivel arc at a distance $\mathbf{u}$ from the shoulder joint. The position of the elbow joint expressed in the frame U is simply determined as $\mathbf{e}_\mathsf{U} = [\rho\ 0\ 0]^T$. Using the vectors that form the local basis, the transformation matrix between the local frame U, and the base coordinate system S, can be determined as

$$\mathsf{U} = \begin{bmatrix} \mathbf{x}_u & \mathbf{y}_u & \mathbf{z}_u & \mathbf{u} \\ 0 & 0 & 0 & 1 \end{bmatrix}. \tag{21}$$

Using the transformation matrix U and the elbow position expressed in the local frame, $\mathbf{e}_\mathsf{U}$, the elbow position in the base coordinate frame S can be computed as

$$\begin{bmatrix} \mathbf{e} \\ 1 \end{bmatrix} = \mathsf{U} \begin{bmatrix} \mathbf{e}_\mathsf{U} \\ 1 \end{bmatrix}. \tag{22}$$

Having just computed the elbow position, it is now possible to determine the arm inverse kinematics. In order to compute the shoulder angles, a transformation matrix between the shoulder and the elbow coordinate frames E will be analyzed:

$$\mathsf{E} = \begin{bmatrix} e_{11} & -s1c2 & e_{13} & l_u s1c2 \\ e_{21} & c1c2 & e_{23} & -l_u c1c2 \\ -c2c3 & s2 & c2s3 & -l_u s2 \\ 0 & 0 & 0 & 1 \end{bmatrix}, \tag{23}$$

where $s1 = \sin q_1$, $s2 = \sin q_2$, $s3 = \sin q_3$, $c1 = \cos q_1$, $c2 = \cos q_2$ and $c3 = \cos q_3$. Expressions for some elements of matrix E were omitted due to their complexity and their insignificant role in computing the shoulder angles. On the other hand, matrix E can also be formed with the vectors forming the coordinate frame of the upper arm as (see Fig. 1 and Fig. 2)

$$\mathsf{E} = \begin{bmatrix} \mathbf{x}_3 & \mathbf{y}_3 & \mathbf{z}_3 & \mathbf{e} \\ 0 & 0 & 0 & 1 \end{bmatrix}, \tag{24}$$

where

$$\begin{aligned} \mathbf{y}_3 &= \frac{\mathbf{e} - \mathbf{s}}{\|\mathbf{e} - \mathbf{s}\|}, \\ \mathbf{z}_3 &= \frac{(\mathbf{e} - \mathbf{s}) \times (\mathbf{w} - \mathbf{s})}{\|(\mathbf{e} - \mathbf{s}) \times (\mathbf{w} - \mathbf{s})\|}, \\ \mathbf{x}_3 &= \frac{\mathbf{y}_3 \times \mathbf{z}_3}{\|\mathbf{y}_3 \times \mathbf{z}_3\|}. \end{aligned} \tag{25}$$

By comparing equations (23) and (24) it is possible to estimate the shoulder angles as

$$\begin{aligned} q_1 &= \arctan \frac{-{}^{(1)}\mathbf{y}_3}{{}^{(2)}\mathbf{y}_3}, \\ q_2 &= \arcsin {}^{(3)}\mathbf{y}_3, \\ q_3 &= \arctan \frac{{}^{(3)}\mathbf{z}_3}{{}^{(3)}\mathbf{x}_3}, \end{aligned} \tag{26}$$

where arctan is a four quadrant inverse tangent function.

Since the elbow joint variable q_4 represents the only joint variable that affects the distance $\|\mathbf{w} - \mathbf{s}\|$, q_4 can be computed independently. We consider the normal vector of the plane containing the shoulder, elbow and wrist joints parallel to the elbow axis of rotation. Therefore angle q_4 can be estimated trivially using the law of cosines as

$$q_4 = \arcsin \frac{l_u^2 + l_f^2 - \|\mathbf{w} - \mathbf{s}\|^2}{2 l_u l_f}. \tag{27}$$

At this point only wrist angles still remain to be estimated. Since the position and the orientation of the hand is measured directly through the direct kinematic model of the robot, the transformation matrix H is known. Using the already estimated shoulder and elbow angles, are first computed transformation matrices T_s from (1) and T_e from (2). The wrist joint transformation matrix $\mathsf{T}_w = f(q_5, q_6, q_7)$ can accordingly be computed as

$$\mathsf{T}_w = (\mathsf{T}_s \mathsf{T}_e)^{-1} \mathsf{H}. \tag{28}$$

In order to determine the wrist angles, the matrix T_w in (3) is rewritten in an analytical form as

$$\mathsf{T}_w = \begin{bmatrix} t_{11} & -\sin q_5 \cos q_6 & t_{13} & 0 \\ t_{21} & \cos q_5 \cos q_6 & t_{23} & 0 \\ -\cos q_6 \sin q_7 & \sin q_6 & \cos q_6 \cos q_7 & 0 \\ 0 & 0 & 0 & 1 \end{bmatrix}, \tag{29}$$

where expressions for some elements of matrix T_w were omitted due to their complexity and their insignificant role in computing the wrist angles. By observing the matrix T_w and considering (28), it is now possible to estimate wrist angles as

$$\begin{aligned} q_5 &= \arctan \frac{-t_{12}}{t_{22}}, \\ q_6 &= \arcsin t_{32}, \\ q_7 &= \arctan \frac{-t_{31}}{t_{33}}. \end{aligned} \tag{30}$$

II.2. Experimental setup

The performance of the system utilizing derived calculation approach was evaluated on two intact volunteers. The experimental setup is shown in Fig. 3. Two 2–axis

https://doi.org/10.1017/S0263574705002304 Published online by Cambridge University Press



Fig. 3. Experimental setup – robot Staubli RX90B with JR3 force sensor, accelerometers attached to the upper arm, and OPTOTRAK infrared markers on the arm, hand, and robot handle.

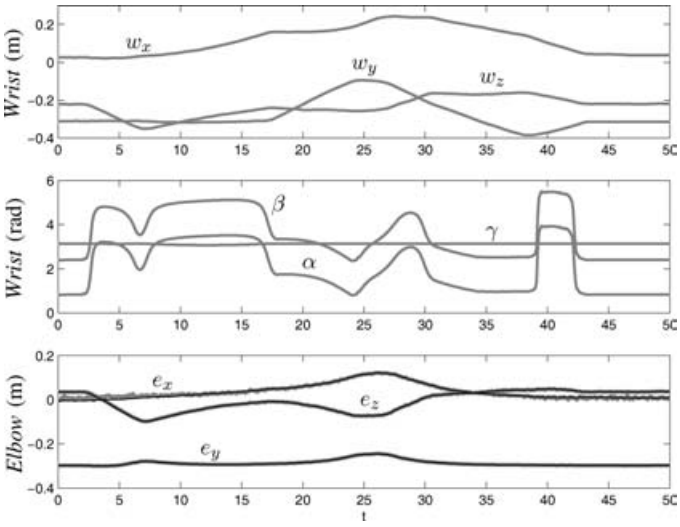


Fig. 4. The first two plots show wrist position and orientation (expressed in terms of ZYZ Euler angles) relative to the shoulder coordinate system. The third plot presents the estimated and measured elbow position (estimated – thick gray line, reference – thin black line).

accelerometers ADXL202 (Analog Device, Inc.) were attached to the subject's upper arm at a distance of 80 mm between each other. Two sets of tests were accomplished. In the first set the subject's arm was moved through a predefined trajectory with the Staubli RX90B robot (Staubli Faverges SCA). The movement was accomplished with velocities ranging from 3% to 45% of the robot maximal velocity which is approximately 1.5 m/s.

For the second set of tests the robot was programmed to behave like a haptic device to generate no resistance to subject's voluntary arm movements. A six axis force/torque sensor (JR3 Inc.) was used for measuring interaction forces between the human and the robot. An impedance controller running on RTLinux operating system with 4 kHz sampling frequency enabled robot movement without resistance. In this way was the subject allowed to move the robot with minimal arm force. The robot position data and accelerometer data were sampled at 4 kHz and filtered using Kalman filter.

Independently were the position and the orientation of the arm and hand measured using the contactless position acquisition system OPTOTRAK with infrared markers that were placed on the shoulder, elbow, and wrist joints as well as on the first joint of the first and the little fingers. The subject was initially sited in a position where all arm angles were zero (as in Fig. 1) when holding the tool mounted on the robot. In this way could the shoulder position be determined from the robot end-effector pose and upper arm and forearm lengths estimated from the OPTOTRAK data.

III. RESULTS

Fig. 4 shows wrist and elbow trajectories for a typical movement when human arm was moved through a predefined path. The first plot indicates wrist position determined from the robot tool pose and the second plot presents hand orientation in terms of ZYZ Euler angles. Wrist pose is defined relatively to the shoulder coordinate system S. The third graph in Fig. 4 shows the estimated position of the elbow joint (thick gray line) as well as the elbow position measured using the OPTOTRAK system (thin black line). It can be noticed that the estimation error for the e_y coordinate of the elbow position, which is directly calculated from acceleration measurements based on (13) is negligible. The error can generally be attributed to the shoulder movement and the inaccurate estimation of the upper arm length, since markers attached to the skin tend to move. If the e_y coordinate is estimated correctly, also coordinates e_x and e_z are reliable since only small errors are expected in the estimation of the hand pose from robot kinematic data.

Figure 5 shows the estimated and measured shoulder, elbow and wrist joints angles for four different movement velocities. The *very slow movement* was accomplished with 3% of the robot maximal joint velocity, the *slow movement* with 15%, the *fast movement* with 30%, while the *very fast movement* was accomplished with 45% of the robot maximal joint velocity. The *fast* and *very fast* movements were noticeably to fast for any human-robot interaction, especially if meant for rehabilitation purposes. Nevertheless, we used the high velocity movements in the experiments to show that the measurement of joint angles is not sensitive to acceleration dynamic components.

Accelerometer signals are generally too noisy for estimation purposes without prior filtering. However, the noise reflected in the estimated shoulder angles was relatively low and could be further reduced using the Kalman filter. Since the accelerometer measurements were not used for the estimation of the elbow angle, q_4, the estimation of this angle was noise free. The noise was again reflected in the estimation of the wrist angles, since the computation of matrix T_w requires employment of noisy shoulder angle trajectories. Nevertheless, with the implementation of the Kalman filter the sensor noise could be attenuated to satisfy the angle estimation requirements as demonstrated by the following analysis.

Figure 6 shows average root-mean-square (RMS) errors for all seven arm joint angles based on 28 measurements

https://doi.org/10.1017/S0263574705002304 Published online by Cambridge University Press

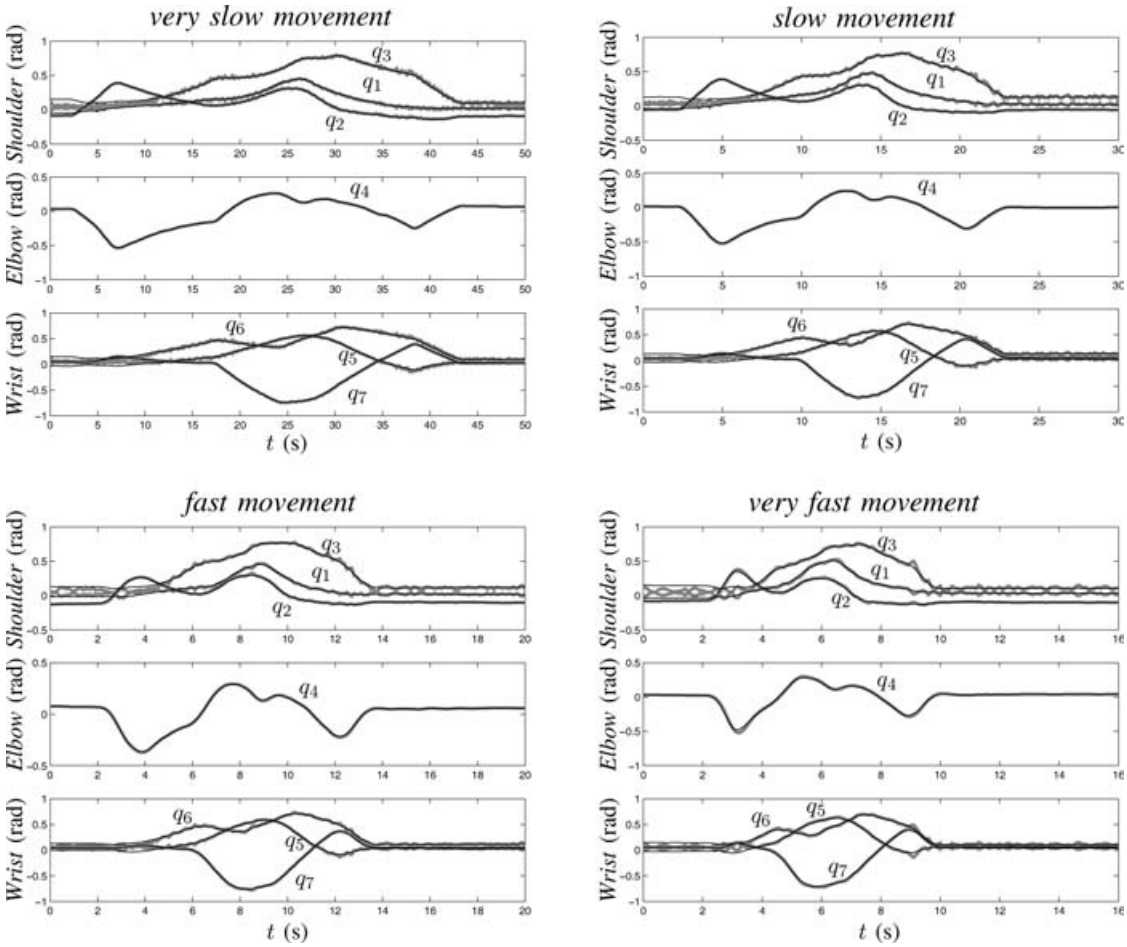


Fig. 5. Estimated and measured arm angles (estimated – thick gray line, reference – thin black line).

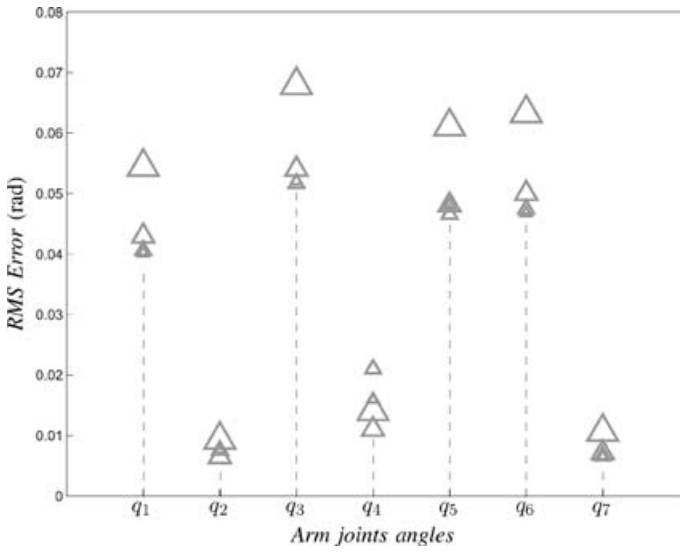


Fig. 6. Average root-mean-square (RMS) errors for estimated arm joint angles based on 7 measurements for each movement velocity. Larger △ indicates RMS error for higher movement velocity.

(7 trials for each movement velocity). The smallest errors were observed for angles q_2, q_4, and q_7. Low RMS error for q_4 is justified by the fact that acceleration measurements are not required for its estimation. Relatively low estimation errors for angles q_2 and q_7 are the result of the arm posture during testing. Namely, the estimation output depends on the accelerometer data as well as hand pose measurements and the propagation of the accelerometer noise to the estimates of arm angles depends on the arm posture.

However, even though it is not possible to generalize the low estimation error for q_2 and q_7 for all arm configurations, the error was found relatively constant for arm postures attainable during robot based rehabilitation. For other joint angles the observed RMS errors were higher, however within 5° margins. Such error margins should be acceptable for most applications, since the residual shoulder movement, geometry or arm joints, movement of soft tissue and complex shape of arm segments limit the measuring accuracy. The estimation error generally increases with the increased movement velocity. However, the observed changes are not substantial considering the extremely high robot movement velocity in the last experiments.

Figure 7 shows the result of the second test which consisted of a free arm movement. Shown are wrist position and orientation determined on the basis of robot direct kinematic model on first two plots and estimated as well as measured arm joint angles on last three plots. The thin dotted lines show the results of the estimation process without any prefiltering. It can be observed that estimated signals are relatively noisy and would therefore be useless. However, the filtered estimated values are close to the measured angles with the estimation errors in the same range as in Fig. 6.

https://doi.org/10.1017/S0263574705002304 Published online by Cambridge University Press

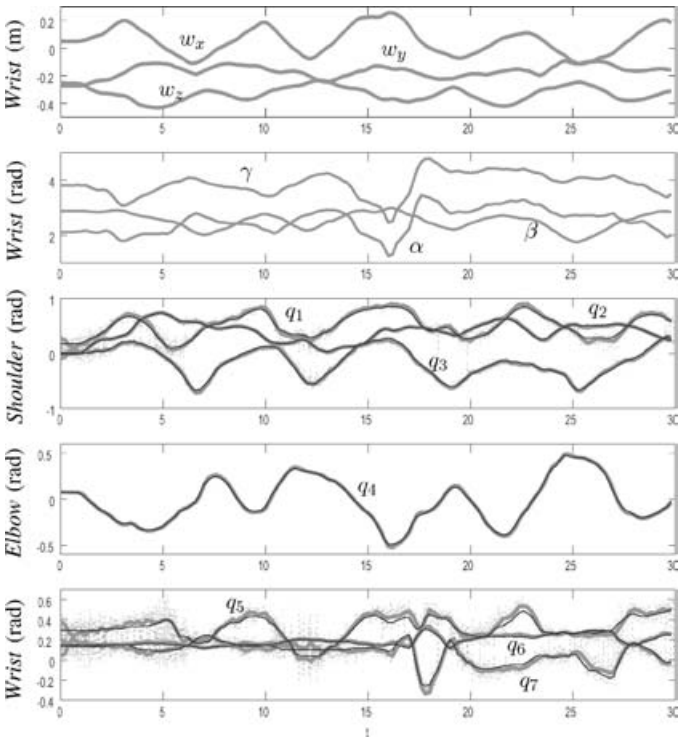


Fig. 7. Arm free movement; wrist position and orientation (in terms of ZYZ Euler angles); estimated and measured shoulder, elbow and wrist angles (without prefiltering – dotted line, Kalman filter output – thick gray line, reference – thin black line).

IV. SUMMARY AND CONCLUSIONS

The paper depicts a technique for computation of the inverse kinematic model of the human arm. The approach is based on measurements of the hand position and orientation and radial acceleration of the upper arm. The algorithm gives sufficiently good estimates of the human arm angles, for use in trajectory planning for rehabilitation purposes, for evaluation of movement capabilities of patients with movement disorders and in control algorithms for artificial activation of upper extremity muscles using FES or exoskeleton devices.

The most limiting factor in the implementation of the inverse kinematics algorithm is required fixation of the shoulder joint. Having in mind that is the subject during upper extremity rehabilitation usually sited, the fixation of the shoulder joint can simply be accomplished by using belts that are attached to the back of the chair.

Analytical and empirical analysis showed that the simplified equation (10) yields adequate results for most applications in robot assisted rehabilitation and assessment where relatively slow robot movement is required. However, if faster movements are necessary a more general solution based on two accelerometers that allow elimination of dynamic acceleration components can be used as in equation (11).

The algorithm and the results presented in this paper prove the feasibility of the inverse kinematic model computation of the human arm that is based on hand pose and upper arm radial acceleration measurements. The algorithm is simple and numerically robust to the noise being present in the acquired accelerometer data. The algorithm was validated with the use of Staubli RX90B robot, however the system may be applicable in most tasks where rehabilitation robots or haptic interfaces are used.

Acknowledgment

Authors would like to thank Ministry of Education, Science and Sport of Republic of Slovenia for their financial support.

References

1. N. Tejima, "Rehabilitation robotics: a review," *Adv. Robot.* **14**, 551–564 (2000).
2. M. Hillman, "Introduction to the special issue on rehabilitation robotics," *Robotica* **16**, Part 5, 485–485 (1998).
3. A. Bardorfer, M. Munih, A. Zupan and A. Primozic, "Upper limb motion analysis using haptic interface," *IEEE/ASME Trans. Mechatron.* **6**, 253–260 (2001).
4. R. Riener and A. Straube, "Inverse dynamics as a tool for motion analysis: Arm tracking movements in cerebellar patients," *J. Neurosci. Methods* **72**, 87–96 (1997).
5. J. Korein, "A geometric investigation of reach," *Ph.D. dissertation* (University of Pennsylvania, 1985).
6. D. Tolani and N. I. Badler, "Real-time inverse kinematics of the human arm," *Presence* **5**, 393–401 (1996).
7. Y. Koga, K. Kondo, J. Kuffner and J. Latombe, "Planning motions with intentions," *Proc., SIGGRAPH'94*, Orlando, FL (July 24–29, 1994) pp. 395–407.
8. J. F. Soechting and M. Flanders, "Sensorimotor representations for pointing to targets in three dimensional space," *J. Neurophysiology* **62**, 582–594 (1989).
9. R. B. Loftin, J. C. Maida and J. Yang, "Inverse kinematics of the human arm," *Technical report* (University of Houston, Houston, TX, 1997).
10. R. A. Prokopenko, A. A. Frolov, E. V. Biryukova and A. Roby-Brami, "Assessment of the accuracy of a human arm model with seven degrees of freedom," *J. Biomech.* **34**, 177–185 (2001).
11. M. B. Popović, D. B. Popović and R. Tomović, "Control of arm movement: Reaching synergies for neuroprosthesis with life–like control," *Journal of Automatic Control* **12**, 9–15 (2002).
12. D. Tolani, A. Goswami and N. I. Badler, "Real–time inverse kinematics techniques for anthropomorphic limbs," *Graph. Models* **62**, 353–388 (2000).
13. A. T. M. Willemsen, C. Frigo and H. B. K. Boom, "Lower extremity angle measurement with accelerometers – error and sensitivity analysis," *IEEE Trans. Biomed. Eng.* **38**, 1186–1193 (1991).

https://doi.org/10.1017/S0263574705002304 Published online by Cambridge University Press